AIAA JOURNAL
Vol. 42, No. 12, December 2004

# Technical Notes

*TECHNICAL NOTES are short manuscripts describing new developments or important results of a preliminary nature. These Notes cannot exceed six manuscript pages and three figures; a page of text may be substituted for a figure and vice versa. After informal review by the editors, they may be published within a few months of the date of receipt. Style requirements are the same as for regular contributions (see inside back cover).*

## Prediction of Sound from Flow over Circular Cylinder Using Modified Green Function

Giwoong Yun* and Haecheon Choi†
*Seoul National University, Seoul 151-744, Republic of Korea*
and
Dongshin Shin‡
*Hongik University, Seoul 121-791, Republic of Korea*

### Nomenclature

| | | |
|---|---|---|
| $c_\infty$ | = | sound speed |
| D/D$t$ | = | $\partial/\partial t + \partial/\partial x_1$ |
| $d$ | = | cylinder diameter |
| $G$ | = | Green function |
| $H_0^{(2)}$ | = | Hankel function of the second kind of zeroth order |
| $I_m$ | = | modified Bessel function of the first kind of integer order $m$ |
| $I'_m$ | = | derivative of $I_m$ |
| $K_m$ | = | modified Bessel function of the second kind of integer order $m$ |
| $K'_m$ | = | derivative of $K_m$ |
| $k$ | = | $\omega/c_\infty$ |
| $M$ | = | freestream Mach number, $= u_\infty/c_\infty$ |
| $n$ | = | azimuthal wave number |
| $n_j$ | = | directional cosine of the outward normal to a solid surface |
| $P_{ij}$ | = | $p\delta_{ij} - \tau_{ij}$ |
| $p$ | = | pressure |
| $R$ | = | cylinder radius |
| $Re$ | = | Reynolds number, $= u_\infty d/\nu$ |
| $r$ | = | $\lvert\bar{r}\rvert = \lvert\bar{x} - \bar{y}\rvert$ |
| $T_{ij}$ | = | Lighthill stress tensor, $= \rho u'_i u'_j + \delta_{ij}(p - \rho/M^2) - \tau_{ij}$ |
| $t$ | = | time |
| $t^*$ | = | retarded time, $= t - Mx\cosh\xi$ |
| $u_i$ | = | velocity |
| $u'_i$ | = | $u_i - \delta_{i1}$ |
| $u_\infty$ | = | freestream velocity |
| $x$ | = | $\sqrt{(x_1^2 + x_2^2)}$ |
| $\bar{x}$ | = | observation-point position vector, $= (x_1, x_2) = (r_x, \theta_x)$ |
| $y_1$ | = | direction of the freestream velocity |
| $y_2$ | = | direction normal to $y_1$ |
| $\bar{y}$ | = | source-point position vector, $= (y_1, y_2) = (r_y, \theta_y)$ |
| $\gamma^2$ | = | $-\omega^2/c_\infty^2$ |
| $\partial\Omega$ | = | cylinder surface |
| $\nu$ | = | kinematic viscosity |
| $\xi$ | = | integration variable of the Hankel function |
| $\rho$ | = | density |
| $\rho'\lvert_D$ | = | acoustic density fluctuations from the body-force fluctuations |
| $\rho'\lvert_Q$ | = | acoustic density fluctuations from the velocity fluctuations in the wake |
| $\tau_{ij}$ | = | viscous stress tensor, $= (\partial u'_i/\partial x_j + \partial u'_j/\partial x_i - \frac{2}{3}\delta_{ij}\partial u'_k/\partial x_k)/Re$ |
| $\Omega$ | = | computational domain for the near-field velocity and pressure |
| $\omega$ | = | frequency |

Received 20 October 2003; revision received 27 May 2004; accepted for publication 4 August 2004. 

*Graduate Student, School of Mechanical and Aerospace Engineering.
†Professor, School of Mechanical and Aerospace Engineering; choi@socrates.snu.ac.kr. Senior Member AIAA.
‡Associate Professor, Department of Mechanical Engineering.

### I. Introduction

VORTEX shedding observed in the wake behind a circular cylinder increases the mean drag and the drag and lift fluctuations. These body-force fluctuations and the velocity fluctuations in the wake are the main sources of the flow-induced sound from a circular cylinder: the drag and lift fluctuations generate a dipole sound, and the unsteady wake generates a quadrupole sound.

So far, two different approaches have been mostly taken to estimate the sound propagation from flow over a circular cylinder at low Mach numbers. One is to solve the unsteady compressible Navier–Stokes equations using a high-order scheme in space and time and directly obtain both the flow and sound fields.[1] The other is to solve the unsteady incompressible Navier–Stokes equations using a low-order (mostly second-order) scheme in space and time and apply the Lighthill's acoustic analogy[2] to obtain the sound field.[3–6] In the latter approach, the far-field and compact-source approximations have been often used to predict the far-field sound propagation, assuming that the distance between observation and source points is larger than the acoustic wavelength and the solid body and the source region are smaller than the acoustic wavelength. Also, using the Curle's formulation[3] of the Lighthill's acoustic analogy, one can estimate the contributions from the body-force and velocity fluctuations to the overall far-field sound, respectively.

The accuracy of predicting the far-field sound using the acoustic analogy has been shown for various flows by comparison with the direct solution of sound field, for example, corotating vortex pair,[7] mixing layer,[8,9] vortex pairing in a jet,[10] turbulent jet,[11,12] and isotropic turbulence.[13] Especially, for flow over a circular cylinder, Inoue and Hatakeyama[1] compared the direct solution of the compressible Navier–Stokes equations with the solution from the acoustic analogy with the far-field and compact-source approximations and showed that the Curle's solution well describes the sound propagation.

On the other hand, in the case of near-field sound all of the previous studies have been conducted using the first approach, that is, direct simulation of compressible Navier–Stokes equations. With this approach, however, it is difficult to estimate whether the near-field sound from flow over a bluff body comes from the body-force fluctuations or from the velocity fluctuations in the wake. For this purpose, we use the second approach based on the acoustic analogy in order to investigate the near-field sound characteristics from flow over a circular cylinder, where the far-field and compact-source

approximations are not valid any more. Also, it might be interesting to compare the overall sound obtained from the present study with that from the direct simulation[1] to see if the second-order scheme used in the present study accurately predicts the near-field sound.

Therefore, in the present study we obtain the near-field sound from the Curle's integral solution using a modified Green function with which the effect of the solid surface on the sound propagation is included. The sound obtained is compared with the direct solution of the compressible Navier–Stokes equations.[1] Also, three different solutions obtained from the acoustic analogy with the modified Green function, free-space Green function and far-field and compact-source approximations, are analyzed in the near field. The importance of the velocity fluctuations in the wake as a source of the near-field sound is finally addressed in this Note.

## II. Acoustic Analogy

The Lighthill acoustic analogy[2] is expressed in a nondimensional form as

$$\frac{\mathrm{D}^2\rho}{\mathrm{D}t^2} - \frac{1}{M^2}\frac{\partial^2\rho}{\partial y_j \partial y_j} = \frac{\partial^2 T_{ij}}{\partial y_i \partial y_j} \tag{1}$$

When the reference frame is fixed on the moving solid body, the Curle's solution[3] of the Lighthill acoustic analogy[2] can be used to obtain the sound field. The acoustic density fluctuation $\rho'$ is obtained in the frequency domain by Fourier transforming Eq. (1) in time and using the Green function method:

$$\hat{\rho}'(\bar{x},\omega) = M^2 \int_{\partial\Omega} n_j \hat{P}_{ij}(\bar{y},\omega)\frac{\partial \hat{G}}{\partial y_i}\,\mathrm{d}\bar{y} + M^2 \int_{\Omega} \hat{T}_{ij}(\bar{y},\omega)\frac{\partial^2 \hat{G}}{\partial y_i \partial y_j}\,\mathrm{d}^2\bar{y} \tag{2}$$

where $\hat{()}$ is the Fourier coefficient. For the flow geometry and coordinate system, see Fig. 1. Equation (2) shows the acoustic density caused by two typical acoustic sources: the first term in the right-hand side of Eq. (2) depicts the acoustic density $(\rho'|_D)$ from the body-force fluctuations, and the second term $(\rho'|_Q)$ from the velocity fluctuations in the wake, respectively.

Dhanak[14] proposed a modified Green function in a three-dimensional space satisfying $\partial G/\partial r_x = 0$ at $r_x = R\,(= d/2)$ and $G$ an outgoing wave at infinity. The modified Green function in a two-dimensional space can be similarly obtained as

$$\hat{\hat{G}}_{\mathrm{MG}}(\bar{x},\bar{y},\omega,n) = \begin{cases} \left[e^{-in\theta_y}\Big/ K'_m(\gamma R)\right] K_m(\gamma r_y)[K'_m(\gamma R) I_m(\gamma r_x) - I'_m(\gamma R) K_m(\gamma r_x)] \\ \qquad \text{for} \quad r_x \le r_y \\ \left[e^{-in\theta_y}\Big/ K'_m(\gamma R)\right] K_m(\gamma r_x)[K'_m(\gamma R) I_m(\gamma r_y) - I'_m(\gamma R) K_m(\gamma r_y)] \\ \qquad \text{for} \quad r_x > r_y \end{cases} \tag{3}$$

Here $\hat{\hat{()}}$ denotes the Fourier coefficient in the frequency-azimuthal wave-number space. The sound propagation in the presence of the cylinder is accurately predicted with this Green function.

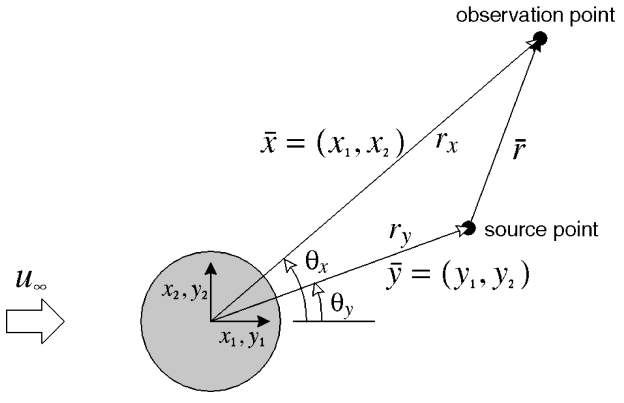


**Fig. 1 Flow geometry and coordinate system.**

The free-space Green function can be used to obtain the sound field when the observation point is apart from the cylinder surface:

$$\hat{G}_{\mathrm{FG}}(\bar{x},\bar{y},\omega) = (i/4)H_0^{(2)}(kr) \tag{4}$$

On the other hand, using the free-space Green function and the far-field and compact-source approximations, the acoustic density fluctuation at the far field is approximated by

$$\rho'_{\mathrm{FC}}(\bar{x},t) = \frac{M^3}{2\pi}\frac{x_i}{x}\int_0^\infty \frac{\partial}{\partial t^*}\int_{\partial\Omega} n_j P_{ij}(\bar{y},t^*)\,\mathrm{d}\bar{y}\,\mathrm{d}\xi + \frac{M^4}{2\pi}\frac{x_i x_j}{x^2}\int_0^\infty \frac{\partial^2}{\partial t^{*2}}\int_{\Omega} T_{ij}(\bar{y},t^*)\,\mathrm{d}^2\bar{y}\,\mathrm{d}\xi \tag{5}$$

In the following section, the subscript FC denotes the acoustic density obtained from the far-field and compact-source approximations [Eq. (5)] and those MG and FG from the modified and free-space Green functions [Eqs. (2) and (3) and Eqs. (2) and (4)], respectively. The Lighthill stress tensor is approximated by the Reynolds-stress term only.[2]

## III. Computational Details

The acoustic source functions in the near flowfield are obtained by solving the unsteady incompressible Navier–Stokes equations in generalized coordinates. The integration method used to solve the equations is based on a fully implicit fractional step method. All terms including cross-derivative diffusion terms are advanced with the Crank–Nicolson method in time and are resolved with the second-order central-difference scheme in space. A Newton method is used to solve the discretized nonlinear equations. The details of the numerical method used in this study are described in Choi et al.[15]

For the near-field velocity and pressure, we use a C-grid system. A Dirichlet boundary condition, $u_1 = 1$ and $u_2 = 0$, is used at far-field computational boundaries, and the no-slip condition is applied on the cylinder surface. The periodic boundary condition is used at the branch cut, and a convective outflow condition is used for the outflow boundary condition. The computational domain size for the near-field velocity and pressure is $-50 \le y_1/d \le 50$ and $-50 \le y_2/d \le 50$, and the number of grid points is $481 \times 121$. The flow at $Re = 150$ is simulated for comparison with the acoustic field obtained from the direct solution[1] of the compressible Navier–Stokes equations. The accuracy of using the present numerical method, grid, computational time step, and boundary conditions was already shown in our previous studies.[5,16]

## IV. Results

At low Mach number, the most dominant acoustic sources are the temporal variations of drag and lift forces on the surface of a cylinder caused by periodic vortex shedding behind the cylinder. The mean drag coefficient $\bar{C}_D = 1.327$, the amplitudes of drag and lift coefficient fluctuations $C'_D = 0.026$ and $C'_L = 0.517$, and the Strouhal number $Sr = 0.183$ are in excellent agreement with those by Inoue and Hatakeyama.[1] Because the lift fluctuations are much larger than the drag fluctuations, it is expected that the intensity of acoustic density by the lift fluctuations is larger than that by the drag fluctuations.

Figures 2a–2c show the contours of the instantaneous acoustic density fluctuations from the body-force fluctuations, velocity fluctuations in the wake, and their sum, respectively, at $Re = 150$ and $M = 0.2$. As expected, the acoustic density caused by the lift fluctuations propagates dominantly in the overall acoustic field. The acoustic density fluctuations caused by the velocity fluctuations appear in the near-wake region and weakly propagate along the directions of $\pm 45$ and $\pm 135$ deg (Fig. 2b).

Inoue and Hatakeyama[1] indicated that in a reference frame fixed to the cylinder one should consider the Doppler effect when the sound field is obtained from the acoustic analogy. That is, the propagation speed $c_\phi(\phi) = c_\infty(1 - M\cos\phi)$ should be used instead of $c_\infty$, where $\phi$ is the angle from the stagnation point. Following Inoue and Hatakeyama,[1] we apply $c_\phi(\phi)$ into $\rho'_{\mathrm{MG}}$, $\rho'_{\mathrm{FG}}$, and $\rho'_{\mathrm{FC}}$. The sound field $\rho'_{\mathrm{MG}}$ with the Doppler effect is shown in Fig. 2d. Because

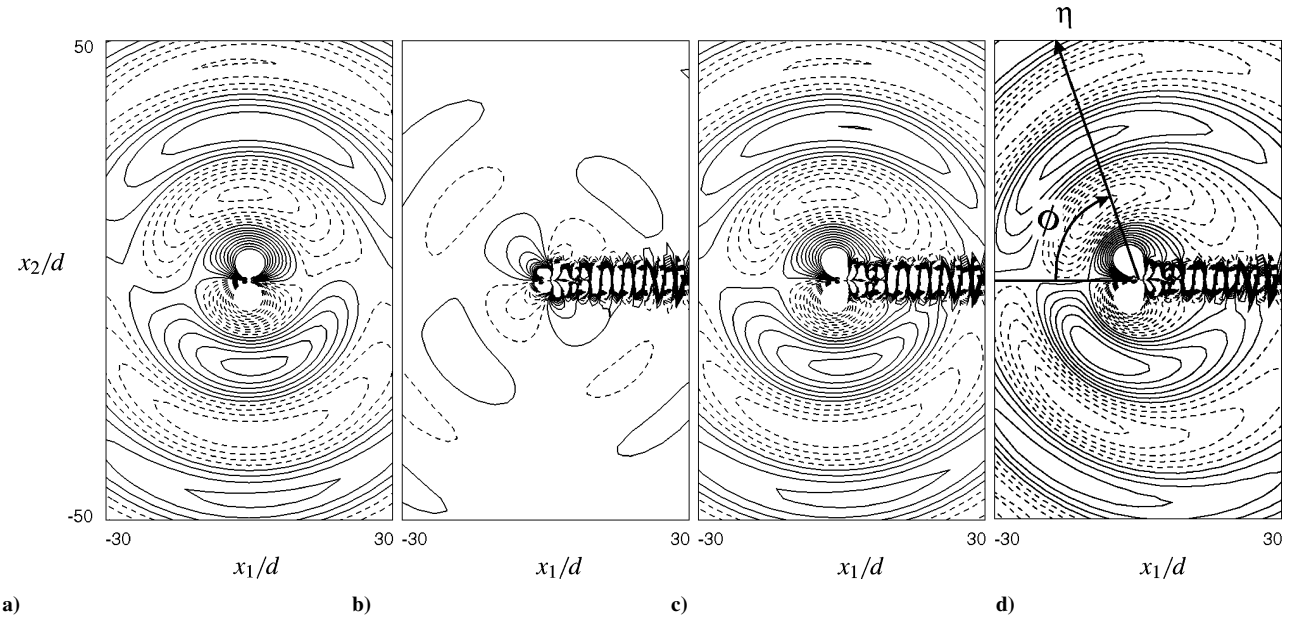


**Fig. 2 Contours of the instantaneous acoustic density fluctuations at $Re = 150$ and $M = 0.2$: a) $\rho'_{MG}|_D$, b) $\rho'_{MG}|_Q$, c) $\rho'_{MG}|_{D+Q}$, and d) $\rho'_{MG}|_{D+Q}$ with the Doppler effect. The contour levels are fixed as $-3.713 \times 10^{-4} \sim 3.713 \times 10^{-4}$. Here, $\eta$ denotes an arbitrary axis for the sound evaluation in Fig. 4.**

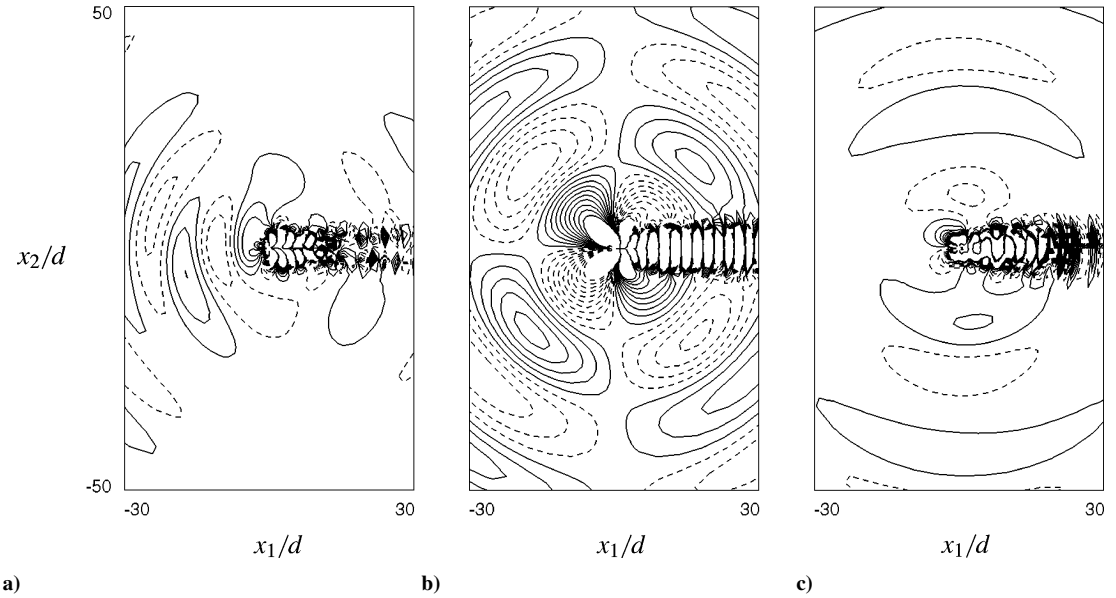


**Fig. 3 Contours of the instantaneous acoustic density fluctuations from the Reynolds-stress components at $Re = 150$ and $M = 0.2$: a) $u'_1u'_1$, b) $u'_1u'_2$, and c) $u'_2u'_2$. Here, the contour levels are fixed as $-3.713 \times 10^{-5} \sim 3.713 \times 10^{-5}$.**

of the Doppler effect, the acoustic density propagates upstream as compared to that in Fig. 2c.

Figure 3 shows the contours of the instantaneous acoustic density fluctuations from $u'_1u'_1$, $u'_1u'_2$, and $u'_2u'_2$. The sound generated from $u'_1u'_2$ is largest among the Reynolds-stress components and propagates along the directions of $\phi = \pm 45$ and $\pm 135$ deg, but those from $u'_1u'_1$ and $u'_2u'_2$ propagate along the directions of $\phi = 0$ and 180 deg and $\phi = \pm 90$ deg, respectively. Therefore, the sound from the velocity fluctuations is basically determined by the Reynolds shear stress (see Figs. 2b and 3). It is interesting to note that the velocity fluctuations in the wake, except those in the vicinity of the cylinder surface, do not radiate the sound into the intermediate or far field.

Figure 4 shows the distribution of the instantaneous $\rho'_{MG}$ with the Doppler effect along the $\eta$ direction at $\phi = 120$ deg (see Fig. 2d), together with those of $\rho'_{FG}$ and $\rho'_{FC}$ with the Doppler effect. These are compared with the direct solution of the compressible Navier–Stokes equations.[1] It is shown in this figure that the overall acoustic

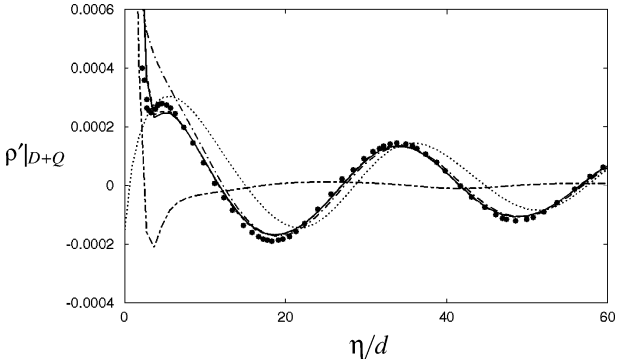


**Fig. 4 Distribution of $\rho'|_{D+Q}$ along the $\eta$ direction at $\phi = 120$ deg for $Re = 150$ and $M = 0.2$: ——, $\rho'_{MG}|_{D+Q}$; – – –, $\rho'_{FG}|_{D+Q}$; · · · ·, $\rho'_{FC}|_{D+Q}$; •, Inoue and Hatakeyama[1]; –·–, $\rho'_{MG}|_D$; and – – –·, $\rho'_{MG}|_Q$.**

density obtained using the modified Green function $\rho'_{MG}|_{D+Q}$ agrees very well with that by Inoue and Hatakeyama,[1] indicating that the acoustic analogy with the modified Green function predicts the near-field sound very accurately. We have also compared $\rho'_{MG}$ at $\phi = 50$ and 78.5 deg with the direct solutions,[1] again showing excellent agreement.

The acoustic density fluctuations generated from the body-force and velocity fluctuations are separately drawn in Fig. 4 to see whether the first is still dominant even in the near field. It is found that the first is dominant for $\eta > 10d$, whereas the latter is also important for $\eta < 10d$. (Note that $\rho'_{MG}|_D$ is quite different from $\rho'_{MG}|_{D+Q}$ there.) Therefore, near the cylinder surface the sound from the velocity fluctuations should not be neglected.

On the other hand, $\rho'_{FG}$ is very similar to $\rho'_{MG}$ even near the cylinder surface at $\phi = 120$ deg, suggesting that the free-space Green function might be preferable in predicting the overall sound to the modified Green function because the latter needs a significant amount of CPU time. As expected, the far-field and compact-source approximations predict very different acoustic density fluctuations near the cylinder surface (Fig. 4).

## V. Conclusions

In the present study, we applied the Lighthill's acoustic analogy[2] to the sound propagation from flow over a circular cylinder at $Re = 150$. To include the effect of the cylinder surface on the sound propagation in the near field, a modified Green function was used. The computed sound was in excellent agreement with the direct solution of the compressible Navier–Stokes equations,[1] supporting the validity of using the acoustic analogy in predicting the near-field sound. Also, three different solutions obtained from the acoustic analogy with the modified Green function, free-space Green function, and far-field and compact-source approximations were analyzed in the near field, showing that the free-space Green function also predicts the acoustic density accurately. Finally, it was shown that the sound from the velocity fluctuations is not negligible in the near field, as compared to that from the body-force fluctuations, as a result of the strong vortex shedding near the cylinder surface.

## Acknowledgment

This work was supported by the Creative Research Initiatives of the Korean Ministry of Science and Technology.

## References

[1]Inoue, O., and Hatakeyama, N., "Sound Generation by a Two-Dimensional Circular Cylinder in a Uniform Flow," *Journal of Fluid Mechanics*, Vol. 471, 2002, pp. 285–314.

[2]Lighthill, M. J., "On Sound Generated Aerodynamically: I. General Theory," *Proceedings of the Royal Society of London, Series A: Mathematical and Physical Sciences*, Vol. 211, No. 1107, 1952, pp. 564–587.

[3]Curle, N., "The Influence of Solid Boundaries upon Aerodynamic Sound," *Proceedings of the Royal Society of London, Series A: Mathematical and Physical Sciences*, Vol. 231, No. 1187, 1955, pp. 505–514.

[4]Hardin, J. C., and Lamkin, S. L., "Aeroacoustic Computation of Cylinder Wake Flow," *AIAA Journal*, Vol. 22, No. 1, 1984, pp. 51–57.

[5]You, D., Choi, H., Choi, M.-R., and Kang, S.-H., "Control of Flow-Induced Noise Behind a Circular Cylinder Using Splitter Plates," *AIAA Journal*, Vol. 36, No. 11, 1998, pp. 1961–1967.

[6]Cox, J. S., Brentner, K. S., and Rumsey, C. L., "Computation of Vortex Shedding and Radiated Sound for a Circular Cylinder: Subcritical to Transcritical Reynolds Numbers," *Theoretical and Computational Fluid Dynamics*, Vol. 12, No. 4, 1998, pp. 233–253.

[7]Mitchell, B. E., Lele, S. K., and Moin, P., "Direct Computation of the Sound from a Compressible Co-Rotating Vortex Pair," *Journal of Fluid Mechanics*, Vol. 285, 1995, pp. 181–202.

[8]Colonius, T., Lele, S. K., and Moin, P., "Sound Generation in a Mixing Layer," *Journal of Fluid Mechanics*, Vol. 330, 1997, pp. 375–409.

[9]Bogey, C., Bailly, C., and Juvé, D., "Numerical Simulation of Sound Generated by Vortex Pairing in a Mixing Layer," *AIAA Journal*, Vol. 38, No. 12, 2000, pp. 2210–2218.

[10]Mitchell, B. E., Lele, S. K., and Moin, P., "Direct Computation of the Sound Generated by Vortex Pairing in an Axisymmetric Jet," *Journal of Fluid Mechanics*, Vol. 383, 1999, pp. 113–142.

[11]Colonius, T., and Freund, J. B., "Application of Lighthill's Equation to a Mach 1.92 Turbulent Jet," *AIAA Journal*, Vol. 38, No. 2, 2000, pp. 368–370.

[12]Freund, J. B., "Noise-Source Turbulence Statistics and the Noise from a Mach 0.9 Jet," *Physics of Fluids*, Vol. 15, No. 6, 2003, pp. 1788–1799.

[13]Whitmire, J., and Sarkar, S., "Validation of Acoustic-Analogy Predictions for Sound Radiated by Turbulence," *Physics of Fluids*, Vol. 12, No. 2, 2000, pp. 381–391.

[14]Dhanak, M. R., "Turbulent Boundary Layer on a Circular Cylinder: the Low-Wavenumber Surface Pressure Spectrum Due to a Low-Mach-Number Flow," *Journal of Fluid Mechanics*, Vol. 191, 1988, pp. 443–464.

[15]Choi, H., Moin, P., and Kim, J., "Turbulent Drag Reduction: Studies of Feedback Control and Flow over Riblets," Dept. of Mechanical Engineering, Stanford Univ., Rept. TF-55, Stanford, CA, Sept. 1992.

[16]Kwon, K., and Choi, H., "Control of Laminar Vortex Shedding Behind a Circular Cylinder Using Splitter Plates," *Physics of Fluids*, Vol. 8, No. 2, 1996, pp. 479–486.

M. Sichel
*Associate Editor*